Comparison of surrogate models for turbomachinery design

J.PETER, M. MARCELET
ONERA
Department of CFD and Aeroacoustics
BP72 – 29 av. De la Div. Leclerc, 92322 Châtillon
FRANCE
jpeter@onera.fr

Abstract: - This article addresses the issue of selecting surrogate models suitable for the global optimization of turbomachinery flows. As a first step towards this goal the analysis of a family of 2D flows on a two-parameter design space is presented. Four types of surrogate models are considered: least square polynomials, artificial neural networks (multi-layer perceptron and radial basis function) and Kriging. Discussed is the ability of these surrogate functions to give a satisfactory description of the exact function of interest on the design space, during a global optimization. The number of CFD evaluations for an adequate description of the exact function is presented

Key-Words: - Turbomachinery, global optimization, surrogate model

Nomenclature

$\alpha = (\alpha_1, \alpha_2)$	Design variable vector
$J(\alpha)$	Exact function of interest
$\bar{J}(\alpha)$	Surrogate model
n_s	Sampling size
J_s	Vector of sampling values
E	Mean square error
$\Psi_i, \Psi_{i,j}$	Polynomial regression coefficients
$\omega = [a_{nm}, ..., b_p]$	Multilayer perceptron weights
$\hat{f}_i$	Radial basis function
r_i	Radius of the radial function
n_c	Number of radial functions
m	Mean value of J
θ	Kriging's correlation parameter
β	Kriging's regression constant
f_i	Kriging's regression function
σ^2	Kriging's variance
Cv	Kriging's covariance function
Err	Mean error on the design space

1 Introduction

Shape optimization is one of the most important applications of computational fluid dynamics (CFD). For example, the drag reduction of an aircraft with constraints on the lift, geometry and momentums is a prominent issue of external aerodynamics. In the field of internal flows, minimization of total-pressure losses of a blade row is an important and classical issue. Despite the huge amount of work devoted to aerodynamic shape optimization during the three last decades, no specific algorithm has appeared to be really adequate for all problems or at least for a very wide range of problems.

Since the mid 70's and the landmark paper of Hicks and VanderPlaats, local optimization using the gradient of functions of interest with respect to the design parameters has focused much attention [31]. In the late 80's and the beginning of the 90's it appeared that those gradients could be computed by the so-called adjoint vector method [14] or direct differentiation method [3] instead of the costly finite difference method. Local optimization of a parameterized solid shape, combining adjoint vector method, a descent method – like feasible descent [30] – and some kind of mesh deformation tool became very popular. ONERA has developed both discrete adjoint vector and discrete direct method in the aerodynamic code *elsA* [5, 19, 20], and demonstrated its ability to carry out optimization of 3D industrial configurations [26]. In other respects, several authors considered the issue of global aerodynamic optimization. Almost all types of global optimization strategies were considered with a significant emphasis on genetic algorithms [9]. The authors interested in this method had to face the bottleneck of the huge cost of the numerous exact evaluations of design requested by the optimization algorithm.

To circumvent this issue, since the mid 1990's many authors replaced some of the exact

evaluations (by the CFD and post-processing codes) by those provided by a well defined surrogate-model. Baron published a review in 1994 dealing with polynomial, spline, radial basis function, kernel smoothing and Kriging (called spatial correlation) metamodel [2]. In 2000, Jin et al. published a description of almost the same types of surrogate models and also a comparison of their efficiency for mathematical functions [15]. One year later, Simpson et al. wrote a broad survey about the use of metamodels including description of response surfaces, neural networks, Kriging and references to articles describing less popular types of surrogate functions [27]. Van Beers and Kleijen published in 2004 a specific survey for Kriging method [4]. At last, Queipo et al. wrote very recently a review including considerations on polynomial regression, Kriging and radial basis function metamodels. Also included are descriptions of several designs of experiments and surrogate based strategies [22].

In other respect, several recent publications deal with the assessment of surrogate functions for actual aerodynamic optimizations. The metamodel is used by some authors to provide inexpensive function evaluations to a genetic algorithm in charge of the optimization process. Demeulaere and Pierret associated a multilayer-perceptron network and a genetic algorithm for the optimization of a 3D compressor blade with 9 design parameters [7]. Giannacoglou and coworkers have numerous contributions to this subject: [10] considers radial basis and multi-layer neural networks, [11] describes how to take into account gradient information in this network. The latter also presents optimization of a 3D turbine blade with Euler equations. Polini et al. described the global optimization of wing with Euler or thin-layer Navier-Stokes equations using 24 parameters. The optimization process involves both a genetic algorithm and Kriging [21]. In many other publications, the i9nexpensive evaluations of the metamodel are used for the global optimization. Giu8nta et al. considered rational and polynomial functions for the global optimization (2 design variables) of a HSCT plane [12]. In 1999, Papila et al. assessed neural networks and polynomial regression for potential flows around an airfoil and a wing (2 design variables) [18]. Rai et al. carried out the global optimization of a 2D turbine airfoil (3 to 15 design variables) combining response surfaces and artificial neural networks [23]. Simpson et al. optimized a nozzle with structural and aerodynamic criteria (considering finite elements for elasticity and Euler equations) with polynomial response surfaces and Kriging model (2 design variables) [28]. More recently Jouhault et al. presented the global optimization of an airfoil with RANS equations using Kriging (2 design variables) [16].

Our work is related to those quoted in the second part of the previous paragraph. Our goal is to assess the use of metamodels for actual aerodynamic optimizations, but not only for one or two classes of surrogates but for four among the most widely used. We focus on the actual search of the most adapted surrogate model for turbomachinery design optimization problem. The article is organized as follows. Geometry, governing equations and design space are presented in section 2. The surrogate models we consider are detailed in section 3. The ability of these surrogate functions to give a satisfactory description of the exact function of interest on the design space is discussed in section 4.

2 Description and Analysis of the Turbomachinery Flow

2.1 Nominal Geometry

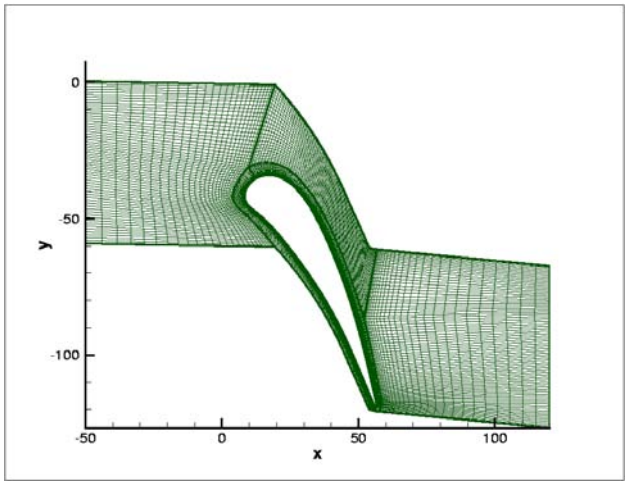

Figure 1: mesh of nominal 2D configuration.

The considered test case is derived from the stator blade of VEGA2 configuration, which is a classical stator rotor turbine configuration [6]. Due to the high cost of global optimization, only a 2D geometry deduced from a n appropriate projection of the 3D geometry at the hub, is studied. The 4 domains mesh with matching joins is presented in figure 2, where the characteristics length of the blade, L = 90mm, can be measured. The total number of mesh points is 11,816. Periodicity conditions are applied at the lower and upper borders. The aerodynamic data of the subsonic inlet are T_i = 288.27 K, p_i = 101,325 Pa. the direction of

the flow at the inlet is also constrained along the *x* axis. At the outlet the static pressure is fixed. Its ratio to the inlet total pressure is $p_{s\ exit}/p_i = 0.35$. The eddy viscosity is determined by Sutherland law. The Reynolds number of the flow based on the stagnation condition is then $Re = \rho_i a_i L/\mu(T_i) = 2.09\ 10^5$.

2.2 Flow Computation

The Reynolds averaged Navier-Stokes equations are considered. The turbulent viscosity is computed by the Smith k-l model [29]. The seven-equation non-linear system is solved numerically by the ONERA finite-volume cell-centered code for structured meshes, called *elsA* [5]. Second order Roe-flux (using MUSCL approach with Van Albada limiting function) is used for mean flow convective term, the first order Roe flux is used for turbulent variable convective term, centered fluxes with interface centered evaluation of gradients are used for both diffusive terms. Centered formula is used for the source term of turbulent variables equations. More details can be found in [24], which also indicates a good comparison with experimental data for the original 3D geometry.

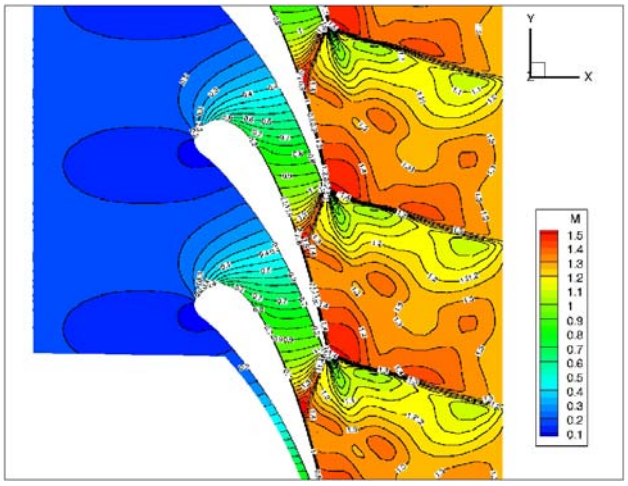

Figure 2: iso Mach-number lines of nominal 2D configuration.

Due to the low value of the static pressure at the exit, the flow is sonic at the narrowest section between two blades, near the trailing edge (just like in a shocked nozzle). Two strong shock lines (one going along the *x* axis, the other oblique) start from the trailing edge of the blade. A view of the iso-Mach number lines is presented.

2.3 Design Space

The geometric deformation of the blade consists in moving the trailing edge along both *x* and *y* axis. The leading edge is fixed. The deformed shape of the blade is defined by a smooth algebraic function of the curvilinear coordinate. The displacement is damped out from the solid shape to the fixed boundary of the blade domain (see mesh plot). The maximum displacement in each direction is +/- 0.4mm. The displacement along the *x* axis is the first design parameter α_1, the displacement along the *y* axis is the second design parameter α_2. The main output of the comparison is the total pressure at the exit, computed by integration on the exit surface. Its non dimensional value (actual value divided by inlet value) varies from 0.918 to 0.924 on the design space. Of course such low values appear because of the strong shocks. This variation is large enough to define an optimization problem.

A large regular sampling of the design space with 21x21 points is considered. All corresponding flows are computed with exactly the same numerical parameters. The explicit space residual of the scheme is decreased for all design by four to five orders of magnitude for all computations. The plot of the exit total pressure on the design space is presented. It was checked that the variation of total pressure when the design changes corresponds to a change in the strength of the oblique shock.

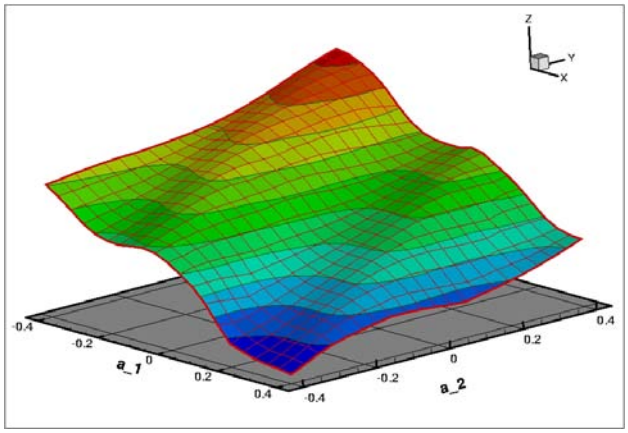

Figure 3: exit total pressure as function of design parameters (axis plane does not correspond to zero).

3 Brief Description of the Surrogate Models

The exact function of interest (exit total pressure for the application) is $J(\alpha)$. The description of the surrogate models is limited to the case of a two-component design vector α. The number of available exact evaluations of the function $J(\alpha)$ is noted n_s. The mean square error (MSE) on the sampling between the exact function $J(\alpha)$ and the surrogate model $\bar{J}(\alpha)$. Is denoted by E.

$$E = \frac{1}{2}\sum_{i=1}^{n_s}(J(\alpha_1^i,\alpha_2^i) - \bar{J}(\alpha_1^i,\alpha_2^i))^2$$

The vector of the exact evaluations is J_s.

$$J_s = [J(\alpha_1),...,J(\alpha_{n_s})]^T$$

3.1 Least Square Polynomial Regression

This method is both simple and well-known. Hence its presentation is limited to a degree two polynomials, although polynomials of degree two, four, six and eight have been considered for the application. Suppose

$$\bar{J}(\alpha) = \Psi_0 + \Psi_1\alpha_1 + \Psi_2\alpha_2 + \Psi_{11}\alpha_1^2 + \Psi_{12}\alpha_1\alpha_2 + \Psi_{22}\alpha_2^2$$

The coefficients of the polynomial are found by minimizing the MSE on the sampling. This leads to

$$\Psi = (X^T X)^{-1} X^T J_s$$

With $\Psi = [\Psi_0\ \Psi_1\ \Psi_2\ \Psi_{11}\ \Psi_{12}\ \Psi_{22}]$ and

$$X = \begin{bmatrix} 1 & \alpha_1^1 & \alpha_2^1 & (\alpha_1^1)^2 & \alpha_1^1\alpha_2^1 & (\alpha_2^1)^2 \\ 1 & \alpha_1^2 & \alpha_2^2 & (\alpha_1^2)^2 & \alpha_1^2\alpha_2^2 & (\alpha_2^2)^2 \\ \vdots & \vdots & \vdots & \vdots & \vdots & \vdots \\ 1 & \alpha_1^{n_s} & \alpha_2^{n_s} & (\alpha_1^{n_s})^2 & \alpha_1^{n_s}\alpha_2^{n_s} & (\alpha_2^{n_s})^2 \end{bmatrix}$$

3.2 Multi-Layer Perceptron

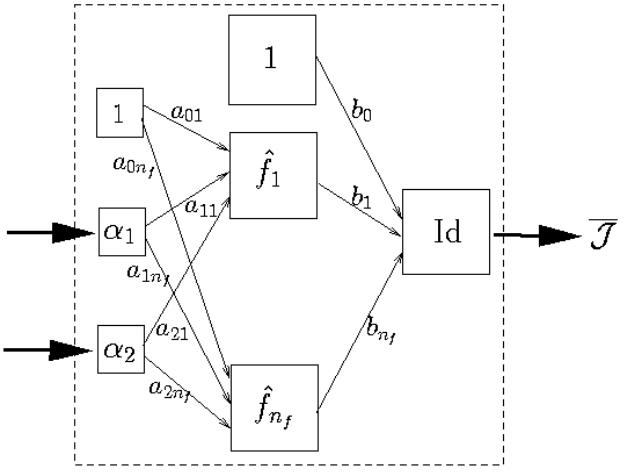

Figure 4: two layer perceptron

Although a wide range of multi-layer perceptrons can be conceived, referring to the universal approximation theorem for neural networks [13], we have decided to use the multi-layer perceptron with just one hidden layer pictured in figure 4. The activation function of the hidden layer units is the sigmoid function and the final output of the network is simply a weighted sum of the hidden layer outputs. A bias value is added to the inputs and to the outputs of the hidden layer.

Given n_s exact computed responses, the $4n_c+1$ unknown coefficients are computed by minimizing the mean square error E.

$$\bar{J}(\alpha_1,\alpha_2) = b_0 + \sum_{j=1}^{n_f} b_j \tanh(a_{0j} + a_{1j}\alpha_1 + a_{2j}\alpha_2)$$

To do so, a steepest descent optimization is performed. Once the gradient of the MSE with respect to the unknown coefficients is calculated, the Wolfe method is used to minimize the MSE in the gradient opposite direction and a new set of coefficients is chosen.

$$\omega^{i+1} = \omega^i - \arg\min_h \left\{ E(\omega_i) - h\frac{dE}{d\omega}(\omega_i) \right\} \frac{dE}{d\omega}(\omega_i)$$

An iterative process is carried out till the value of the gradient of the MSE with respect to the unknown coefficients is equal to zero (according to a user tolerance). The initialization of the unknown coefficients set is an important matter for the method. In the present work, the initial guess of the gradient based search is chosen randomly.

3.3 radial Basis Function Network

The radial basis function network [17] used in this study is composed of n_c radial functions $\hat{f}_i$.

$$\hat{f}_i(\alpha_1,\alpha_2) = \exp\left(-\frac{1}{2}\frac{(\alpha_1 - \alpha_1^i)^2 + (\alpha_2 - \alpha_2^i)^2}{r_i^2} \right)$$

where (α_1^i, α_2^i) and r_i are respectively the centre and the radius of the radial function. The output of the network is given by the following formula:

$$\bar{J}(\alpha_1,\alpha_2) = \sum_{i=1}^{n_c} a_i \hat{f}_i(\alpha_1,\alpha_2)$$

where $A = [a_1, a_2, ..., a_{n_c}]$ is a set of coefficients to determine depending on the exact function to approximate. Given the vector of n_s $(n_s \geq n_c)$ exact values J_s, the minimization of the (MSE) leads to $A = (X^T X)^{-1} X^T J_s$ where X is the following $n_s x n_c$ matrix:

$$X = \begin{bmatrix} \hat{f}_1(\alpha_1^1,\alpha_2^1) & \cdots & \hat{f}_{n_c}(\alpha_1^1,\alpha_2^1) \\ \vdots & \vdots & \vdots \\ \hat{f}_1(\alpha_1^{n_s},\alpha_2^{n_s}) & \cdots & \hat{f}_{n_c}(\alpha_1^{n_s},\alpha_2^{n_s}) \end{bmatrix}$$

Taking the assumption that the number of centers has been fixed, the RBF approximation model is

fully determined once the center and radius of every function is chosen. In this article, every function has the same radius

$$r = \frac{1}{n_c}\left(\max_{1\le i,\, j\le n_s} \sqrt{(\alpha_1^i - \alpha_1^j)^2 + (\alpha_2^i - \alpha_2^j)^2} \right)$$

Moreover, we have picked the radial function centers to coincide with the exact function evaluations points, so that $A = X^{-1} J_s$.

3.4 Simple Kriging

Considering that the value of J at the center of the design space is a good approximation of its mean value *m*, simple Kriging is considered [25]. The statistical basis of the method cannot be described in the limited space of this article. Based on n_s sampling points, the formula of the simple Kriging is a linear interpolation of the known values (applied to $Z(\alpha) = J(\alpha) - m$).

$$\bar{Z}(\alpha) = K_\alpha^T C^{-1} Z_s = Z_s^T C^{-1} K_\alpha$$

(as matrix C is symmetric) with

$$K_\alpha = [C_v(Z(\alpha), Z(\alpha^1)),..., C_v(Z(\alpha), Z(\alpha^{n_s}))]^T$$

$$Z_s = [Z(\alpha^1),..., Z(\alpha^{n_s})]^T \quad \text{and} \quad C = \begin{bmatrix} C_v(Z(\alpha^1), Z(\alpha^1)) & \cdots & C_v(Z(\alpha^{n_s}), Z(\alpha^1)) \\ \vdots & \vdots & \vdots \\ C_v(Z(\alpha^1), Z(\alpha^{n_s})) & \cdots & C_v(Z(\alpha^{n_s}), Z(\alpha^{n_s})) \end{bmatrix}$$

The method is fully defined when the function C_v is selected (it is the covariance of the function Z in the statistical framework of the method description). Most often the following function is chosen $C_v(Z(\alpha^a), Z(\alpha^b)) = \exp(-\theta \parallel \alpha^a - \alpha^b \parallel)$.

The parameter θ is chosen according to a classical heuristic. Its value is determined so that all $\exp(-\theta \parallel \alpha^a - \alpha^b \parallel)$ terms are greater than 0.2.

3.5 Advanced Kriging Methods

In the most general form of the method, called universal Kriging, the approximate function is the sum of a regression and deviation term. The regression is a linear combination on a basis of independent functions

$$f_\alpha = [f_1(\alpha)\ f_2(\alpha) ... f_k(\alpha)]^T$$

The formula of the metamodel is

$$\beta = (F^T C^{-1} F)^{-1} F^T C^{-1} J_s$$

$$\bar{J}(\alpha) = f_\alpha^T \beta + K_\alpha^T C^{-1} (J_s - F\beta)$$

where F is the matrix of the evaluations of the sampling by the f_i functions

$$F = \begin{bmatrix} f_1(\alpha_1) & f_2(\alpha_1) & \cdots & f_k(\alpha_1) \\ \vdots & \vdots & \vdots & \vdots \\ f_1(\alpha_{n_s}) & f_2(\alpha_{n_s}) & \cdots & f_k(\alpha_{n_s}) \end{bmatrix}$$

Moreover, in an advanced stochastic framework, an estimation of Mean Square Error (MSE) of the approximate function is available

$$E(\alpha) = \sigma^2 \left[1 - \begin{bmatrix} f_\alpha^T & K_\alpha^T \end{bmatrix} \begin{bmatrix} 0 & F^T \\ F & C \end{bmatrix} \begin{bmatrix} f_\alpha \\ K_\alpha \end{bmatrix} \right]$$

It can be checked that $E(\alpha)$ is null at sampling points, which is in coherence with the property of data interpolation of Kriging methods. At last a maximum likelihood computation, indicates the optimal value for parameter θ for a given sampling

$$\sigma^2 = \frac{1}{n_s}(J_s - F\beta)^T C^{-1} (J_s - F\beta)$$

$$\beta = (F^T C^{-1} F)^{-1} (F^T C^{-1} F)$$

$$\theta = \arg\min\left[\det(C)^{1/n_s} \sigma^2\right]$$

The benefit of those advanced features of Kriging for the test case of the next section will be discussed in a specific subsection.

4 Evaluations of the Surrogate Model for Design Optimization

The goal of this section is to discuss the efficiency of the surrogate models for the sake of optimization. No optimization tool-box has been used in our study, but our coding relies on a classical linear algebra package – LAPACK [1]. For the studied two-parameter problem, the computation of the surrogate model coefficients can be neglected compared to the cost of one CFD computation. For this reason the efficiency of a surrogate approximation for the optimization problem can be measured by the requested number of exact evaluations.

For all surrogate functions the strategy of sampling enrichment is the same:

A- start with a large enough sampling to determine all coefficients. This initial sampling is built on latin hypercubes

B- add points if criterion (C*) – see below – is not achieved

B1- if the min and max locations of the surrogate model are not all in the sampling then add up four of the missing one

B2- else add to the sampling four points with maximum distance to the points of the sampling

4.1 Definition of the Evaluation Criterion

The function of interest exhibits one global maximum (-0.4,0.4), one local maximum (0.04,0.4), two local minima (-0.2,-0.2), (0.4,0.08) and one global minima (0.4,-0.4) on the 21x21 sample. A surrogate reconstruction will be tested against the following criterion:

(C1) ability to build an approximation with mean error Err on the 21x21 sampling lower than 2 10^{-3}. The mean error Err being adimensioned by the variation of exit static pressure on the design space

$$Err = \frac{\sqrt{\sum_{i,j=1}^{21}\left(p_i(\alpha_1^{ij},\alpha_2^{ij}) - \bar{J}(\alpha_1^{ij},\alpha_2^{ij})\right)^2}}{21^2\left(p_{i\max} - p_{i\min}\right)}$$

(C2) find the global and the local maxima, their location being exact or in a neighboring point of the exact place on the 21x21 sampling

(C3) find the global and the local maxima at the right place on the 21x21 sampling.

The reason for (C2) is that the second order derivatives values are rather low near the maxima so that (C3) is difficult to reach. The results are summarized in Table 1. (IT) indicates the number of exact evaluations needed to satisfy a criterion. Indicated is also the value of Err after 100 CFD computations for all four surrogate models.

Sur. Mod.		C1	IT	C2	IT	C3	IT	Err
3.1 MLP	Pol. 2	KO	-	KO	-	KO	-	2.3 10^{-3}
	Pol. 4	KO	-	KO	-	KO	-	2.1 10^{-3}
	Pol. 6	OK	47	KO	-	KO	-	1.2 10^{-3}
	Pol. 8	OK	53	OK	65	OK	73	4.9 10^{-4}
3.2 Mu. Pe.		OK	300	KO	-	KO	-	2.5 10^{-3}
3.3 RBF		OK	37	OK	38	OK	46	1.6 10^{-3}
3.4 Sim. Kri.		OK	25	OK	62	OK	170	3.7 10^{-4}

Table1: Summary of surrogate model performances.

4.2 Discussion of the Results

From a general point of view, it is clear that RBF (figure 6) and Simple Kriging (figure 5) lead to the best results. Both of them satisfy the (C2) criterion with a reasonable number of exact evaluations. As concerning (C3) only (RBF) and degree-8 polynomial satisfy it with an acceptable number of exact evaluations. The surrogate function surfaces satisfying (C3) are presented in figures 5 and 6. More details are given below concerning the different surrogate models.

- Least square polynomials

Obviously the exact surface cross-sections (α_1=const or α_2=const on figure 3) are much more complicated than parabola, which means that the exact function cannot be well fitted with a second order polynomial. Considering the plots obtained with degree-4 and 6 polynomials, this seems also to be the case.

- Radial basis function

It has also been checked for (RBF) network that the results depend only slightly on the initial six-point sampling

- Multi-layer perceptron

Two multi-layer perceptrons have been tested, respectively with 5 and 10 units in the hidden layer. The first requires almost the whole exact CFD evaluations to satisfy (C1). As for the second, up to 200 evaluations are actually needed. But in spite of the global optima being located from 42 evaluations, none of these perceptrons succeeds in locating the local optima. Besides, from a sampling of 50 evaluations, the computed error does not vary much from 2.4 10^{-3}.

- Simple Kriging

This method leads to the lower error (Err) after a definite number of iterations. Nevertheless it is not the most efficient for the accurate detection of the two maxima.

Sur. Mod.	C1	IT	C20	IT	C3	IT	Err(100)
Sim. K.	OK	25	OK	62	OK	170	3.7 10^{-4}
Ord. K.	OK	25	OK	62	OK	170	3.7 10^{-4}
Uni. $K^{deg\,1}$	OK	28	OK	65	OK	65	3.6 10^{-4}
Uni. $K^{deg\,2}$	OK	28	OK	65	OK	65	3.6 10^{-4}
UK^{d1} MSE	OK	28	OK	57	OK	57	4.1 10^{-4}

Table2: Summary of Kriging metamodel performances.

4.3 Assessment of Advanced Kriging Features

First of all, the benefit of ordinary Kriging – obtained with minimal regression function basis $f_\alpha = [1]$ - and universal Kriging with polynomial regression is studied. Polynomials of degree one and two were considered, $f_\alpha^{\deg 1} = [1, \alpha_1, \alpha_2]$ and

$f_\alpha^{\deg 2} = [1, \alpha_1, \alpha_2, \alpha_1^2, \alpha_1\alpha_2, \alpha_2^2]$ being the corresponding basis. The way those algorithms satisfy the evaluation criterions is summarized in table 2. The performances of the advanced Kriging method on our test case have been observed to be similar to the simple Kriging ones' except for the ability to accurately locate the two maxima (where advanced methods are better).

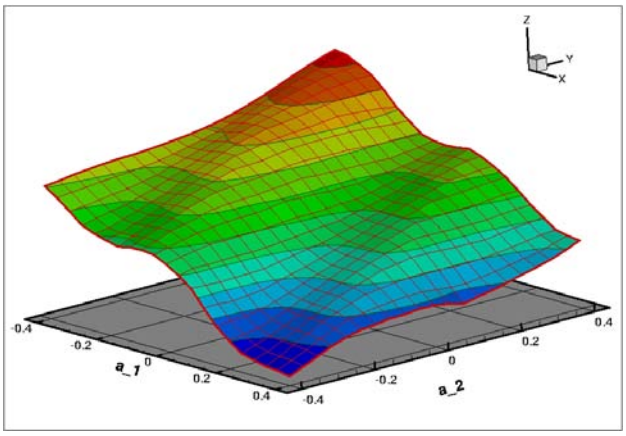

Figure 5: Kriging surface satisfying (C3).

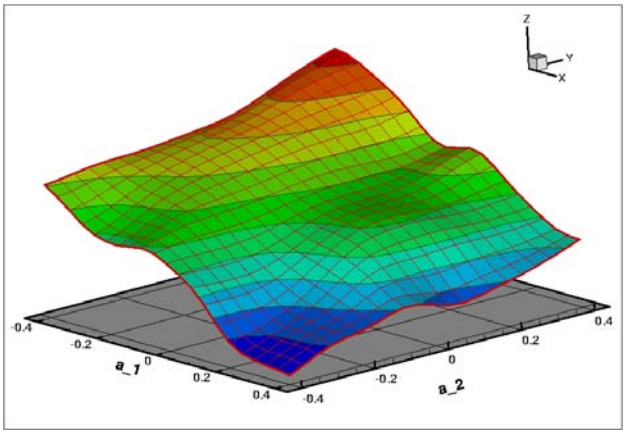

Figure 6: RBF surface satisfying (C3).

The mean square error of the model allows a specific sampling strategy. Step (B2) of the sampling enrichment strategy can be replaced by:
B2K – else add to the sampling the four points with maximum predicted mean square error.

This strategy has been applied to universal Kriging computation with degree one polynomial. For an unknown reason the error after hundred evaluations is slightly increased, but the capability of quickly locating maxima is improved.

At last, some practical trials have been carried out for θ parameter. For all previous computations a value of 2.84 was used, which had been deduced from a common heuristic ("no term in C matrix lower than 0.2"). This value appeared as the upper bound of a very large domain – about [5, 2 10^{-5}] – where the Kriging performances, estimated by all four previous criterions, are almost unchanged. For larger values, approximated functions have almost as many local optimum as sampling points, whereas for very small values of θ, the matrix C is ill-conditioned. Due to those practical considerations, the theoretical optimal value of θ - as defined at the end of section 3.5 – was not computed in this study.

5 Conclusion

This article presented how four types of surrogate models can be used in an industrial context to design a stator blade so as to optimize the local pressure at the exit. Among all the models that have been tested the Kriging models and the radial basis function network appear to give the best results in terms of approximation of the exact function.
In a near future, the gradients of the function of interest with respect to the design variables will also be used as a way to enhance the level of approximation reached by the metamodels. Only a 2D configuration was considered. We also plan to extend the depicted framework to 3d cases.

Acknowledgements: This work was supported by the project NODESIM_CFD "Non-Deterministic Simulation for CFD-based Design Methodologies" funded by the European Community represented by the CEC, Research Directorate-General, in the 6th Framework Program, under Contract No. AST5-CT-2006-030959.

References:

[1] E. Anderson, Z. Bai, C. Bischof, S. Blackford, J. Demmel, J. Dongarra, J. Du Croz, A. Greenbaum, S. Hammarling, A. McKenney, D. Sorensen, *LAPACK Users' Guide*, Third Edition, SIAM, 1999.

[2] R. Barton, Kriging Interpolation in Simulation: a State of Art Review, *Proceedings of the 1994 Winter Simulation Conference*, 1994.

[3] O. Baysal, M. Eleshaky, Aerodynamic Design Sensitivity Analysis Method for the Compressible Euler Equations, *Journal of Fluids Engineering*, Vol.113, No.4, 1991, pp. 681-688.

[4] W. van Beers, J. Kleijnen, Kriging Interpolation in Simulation: a Survey, *Proceedings of the 2004 Winter Simulation Conference*, 2004.

[5] L. Cambier, M. Gazaix, elsA: An Efficient Object-Oriented Solution to CFD Complexity, *AIAA Paper 2002-0108*, 2002.

[6] J. Delery, R. Gaillard, G. Losfeld, C. Pendria, Study of the Iso Cascade in the ONERA S5Ch Wind Tunnel, Pressure Probe and LDV measurement, *ONERA rt 192/1865 DAFE*, 1999.

[7] A. Demeulenaere, S. Pierret, An Integrated Optimization System for Multistage Gas Turbine Design, *Proceedings of Eurogen 2003*, 2003.

[8] G. Dreyfus, J. Martinez, M. Samuelides, M. Gordon, F. Badran, S. Thiria, L. Herault, *Reseaux de Neurones – Methodologie et Applications*, Eyrolles, 2002.

[9] D. Goldberg, *Genetic Algorithms in Search Optimization and Machine Learning*, Addison Weasley, 1989.

[10] K. Giannacoglou, D. Papadimitriou, I. Kampolis, Coupling Evolutionary Algorithms, Surrogate Models and Adjoint Methods in Inverse Design and Optimization Problems, *VKI Lecture Series 2004-07*, 2004.

[11] K. Giannacoglou, D. Papadimitriou, I. Kampolis, Aerodynamic Shape Design Using Evolutionary Algorithms and new Gradient Assisted Metamodels, *Computer Methods in Applied Mechanics and Engineering*, Vol.195, No.44-47, 2006, pp. 6312-6329.

[12] A. Giunta, J. Dudley, R. Narducci, B. Grossman, R. Haftka, W. Mason, L. Watson, Noisy Aerodynamic Response and Smooth Approximations in HSCT Design, *AIAA Paper*, 1994.

[13] K. Hornik, M. Stinchcombe, H. White, Multilayer Feed forward Networks are Universal Approximators, *Neural Networks*, Vol.2, No.5, 1989, pp. 359-366.

[14] A. Jameson, Aerodynamic Design via Control Theory, *Journal of Scientific Computing*, Vol.3, No.3, 1988, pp. 233-260.

[15] R. Jin, W. Chen, T. Simpson, Comparative Studies of Metamodeling Techniques Under Multiple Modeling Criteria, *AIAA Paper 2000-4801*, 2000.

[16] J. Jouhaud, P. Sagaut, M. Montagnac, J. Laurenceau, A Surrogate-Model Based Multidisciplinary Shape Optimization Method Application to a 2D Subsonic Airfoil, *Computers and Fluids*, Vol.36, 2007, pp. 520-529.

[17] M. Orr, *An Introduction to Radial Basis Function Networks*, Center for Cognitive Science, University of Edinburg, Scotland, June 1999.

[18] N. Papila, W. Shyy, N. Fitz-Coy, R. Haftka, Assessment of Neural Network Polynomial Based Techniques for Aerodynamic Applications, *AIAA Paper 99-33401*, 1999.

[19] J. Peter, Discrete Adjoint Method in elsA (part I): Method/Theory, *Proceedings of the 7th ONERA-DLR Aerospace Symposium*, 2006.

[20] J. Peter, F. Drullion, Large Stencil Viscous Flux Linearization for the Simulation of 3D Turbulent Flows with Backward Euler Schemes, *Computers and Fluids*, Vol.36, 2007, pp. 1007-1027.

[21] C. Poloni, P. Loris, L. Larussi, S. Pieri, V. Pediroda, Robust Design of Aircraft Components : a Multi-Objective Optimization Problem, *VKI Lecture Series 2004-07*, 2004.

[22] N. Queipo, R. Haftka, W. Shy, T. Goel, R. Vaidyanathan, P. Tucker, Surrogate-Based Analysis and Optimization, *Progress in Aerospace Sciences*, Vol.41, 2005, pp. 1-28.

[23] M. Rai, N. Madavan, Aerodynamic Design Using Neural Networks, *AIAA Journal*, Vol.38, 2000, pp. 173-182.

[24] F. Renac, C-T. Pham, J. Peter, Sensitivity Analysis for the RANS Equations Coupled with Linearized Turbulence Model, *AIAA Paper 2007-76839*, 2007.

[25] J. Sachs, S. Schiller, W. Welch, Designs for Computer Experiments, *Technometrics*, Vol.31, 1989, pp. 41-47.

[26] I. Salah el Din, G. Carrier, S. Mouton, Discrete Adjoint Method in elsA (part II): Application to Aerodynamic Design Optimization, *Proceedings of 7th ONERA-DLR Aerospace Symposium*, 2006.

[27] T. Simpson, J. Peplinsky, P. Koch, J. Allen, Metamodels for Computer-Based Engineering Design : Survey and Recommendation, *Engineering with Computers*, Vol.17, 2001, pp. 129-150.

[28] T. Simpson, T. Mauery, J. Korte, F. Mistree, Kriging Model for Global Approximation in Simulation Based Multidisciplinary Design Optimization, *AIAA Journal*, Vol.39, 2001, pp. 2233-2241.

[29] B. Smith, A near Wall Model for the k-l Two Equation Turbulence Model, *AIAA Paper 94-2386*, 1994.

[30] G. Vanderplaats, *Numerical Optimization for Engineering Design*, 3rd Ed., VR and D, 1999.

[31] G. Vanderplaats, R. Hicks, Numerical Airfoil Optimization Using a Reduced Number of Design Coordinates, *TMX 73151, NASA*, 1976.